NANO LETTERS

Letter

pubs.acs.org/NanoLett

Gold Nanorods Conjugated Porous Silicon Nanoparticles Encapsulated in Calcium Alginate Nano Hydrogels Using Microemulsion Templates

Hongbo Zhang,[†,‡,∥,▽,○] Yueqi Zhu,[§,▽] Liangliang Qu,[†,‡,▽] Huayin Wu,[‡,▽] Haixin Kong,[▽,†] Zhou Yang,[†] Dong Chen,[‡,◆] Ermei Mäkilä,[⊥] Jarno Salonen,[⊥] Hélder A. Santos,[#] Mingtan Hai,[*,†,‡] and David A. Weitz[*,‡]

[†]Beijing Key Laboratory of Function Materials for Molecule & Structure Construction, School of Materials Science and Engineering, University of Science and Technology Beijing, Beijing 100083, People's Republic of China

[‡]Harvard John A. Paulson School of Engineering and Applied Sciences, Harvard University, Cambridge, Massachusetts 02138, United States

[§]Department of Interventional Radiology, The Sixth Affiliated Hospital of Shanghai Jiaotong University, Shanghai 200233, People's Republic of China

[∥]Pharmaceutical Sciences Laboratory, Turku Center for Biotechnology, Åbo Akademi University, Turku 20520, Finland

[⊥]Laboratory of Industrial Physics, University of Turku, Turku FI-20014, Finland

[#]Division of Pharmaceutical Chemistry and Technology;, Helsinki Institute of Life Science, HiLIFE, University of Helsinki, FI-00014 Helsinki, Finland

S *Supporting Information*

ABSTRACT: Porous silicon nanoparticles (PSiNPs) and gold nanorods (AuNRs) can be used as biocompatible nanocarriers for delivery of therapeutics but undesired leakage makes them inefficient. By encapsulating the PSiNPs and AuNRs in a hydrogel shell, we create a biocompatible functional nanocarrier that enables sustained release of therapeutics. Here, we report the fabrication of AuNRs-conjugated PSi nanoparticles (AuNRsPSiNPs) through two-step chemical reaction for high-capacity loading of hydrophobic and hydrophilic therapeutics with photothermal property. Furthermore, using water-in-oil microemulsion templates, we encapsulate the AuNRsPSiNPs within a calcium alginate hydrogel nanoshell, creating a versatile biocompatible nanocarrier to codeliver therapeutics for biomedical applications. We find that the functionalized nanohydrogel effectively controls the release rate of the therapeutics while maintaining a high loading efficiency and tunable loading ratios. Notably, combinations of therapeutics coloaded in the functionalized nanohydrogels significantly enhance inhibition of multidrug resistance through synergism and promote faster cancer cell death when combined with photothermal therapy. Moreover, the AuNRs can mediate the conversion of near-infrared laser radiation into heat, increasing the release of therapeutics as well as thermally inducing cell damage to promote faster cancer cell death. Our AuNRsPSiNPs functionalized calcium alginate nanohydrogel holds great promise for photothermal combination therapy and other advanced biomedical applications.

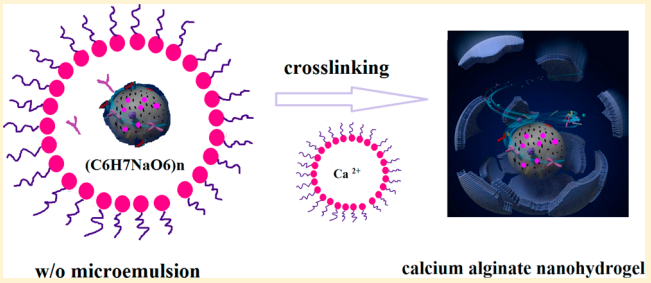

KEYWORDS: *Calcium alginate nano hydrogel, gold nanorods conjugated porous silicon nanoparticles, photothermal therapy, multidrug resistance inhibition, biomedical applications*

Conventional cancer therapy does not distinguish between cancerous and healthy cells in a significant way.[1,2] Fortunately, recent developments such as photothermal therapy has the ability to target the tumor cells and minimize the damage to adjacent normal tissues.[3] Controlled release of therapeutics is another effective way to enhance in vivo therapeutic efficacy, especially when used with synergistic combinations of drugs,[1,2] which inhibit multidrug resistance[3] and reduce side effects.[4] However, creating a single biocompatible nanocarrier that allows high-efficiency coloading of multiple therapeutics, controllable release, and targeted therapy presents a great challenge for encapsulation and release technology.

Porous silicon nanoparticles (PSi NPs)[5−8] are biocompatible and biodegradable nanocarriers for codelivery of therapeutics as

Received: December 11, 2017
Revised: January 25, 2018
Published: January 31, 2018

DOI: 10.1021/acs.nanolett.7b05210
Nano Lett. XXXX, XXX, XXX−XXX

Scheme 1. Formation of Biocompatible Gold Nanorods Conjugated Porous Silicon Nanoparticles Functionalized Calcium Alginate Nanohydrogel Using Water-in-Oil Microemulsion Templates through Crosslinking as a Versatile Therapeutics Co-Delivery Nanocarrier for Photothermal Therapy

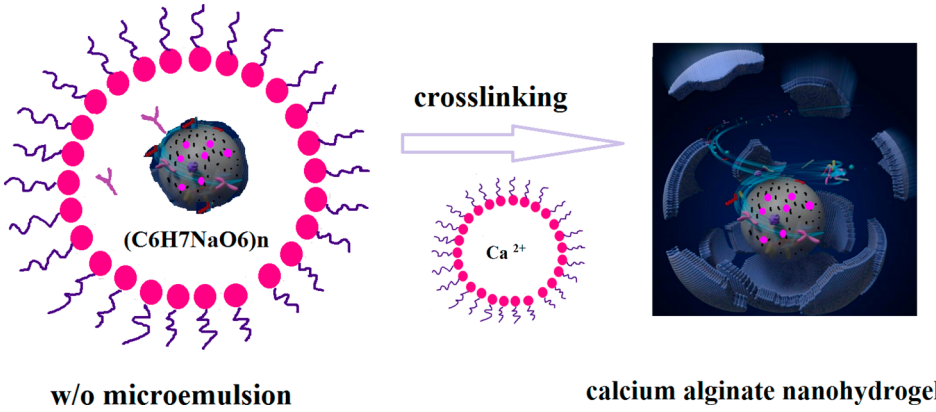

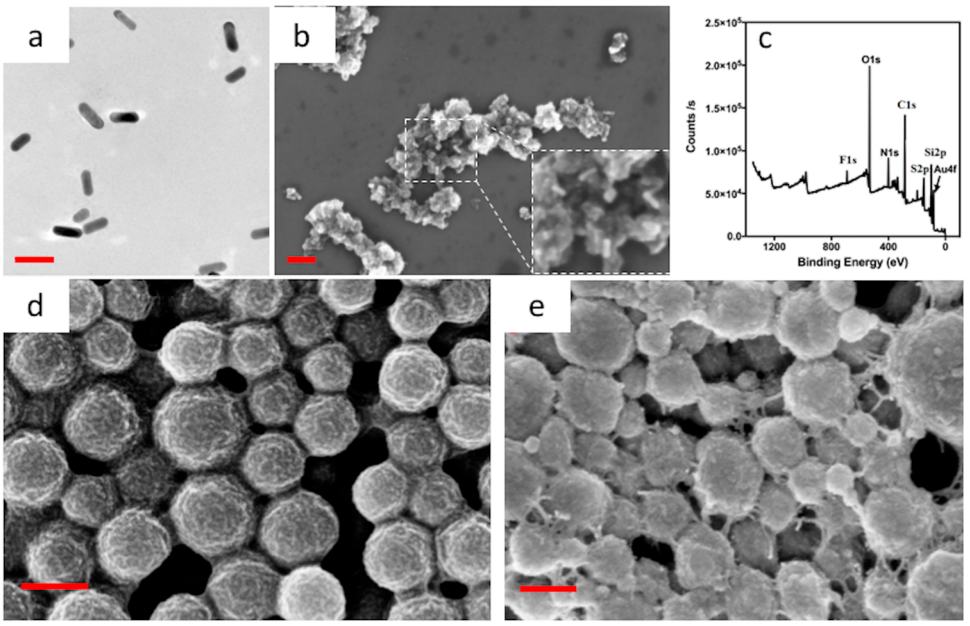

Figure 1. Morphology study of gold nanorods, AuNRsPSiNPs, calcium alginate nanohydrogel and AuNRsPSiNPs functionalized calcium alginate nanohydrogel. (a) TEM image of gold nanorods. The scale bar denotes 50 nm. (b) SEM image of AuNRsPSiNPs. The scale bar denotes 100 nm. (c) XPS spectrum of the gold nanorods conjugated porous silicon nanoparticles. (d) SEM image of calcium alginate nanohydrogel. The scale bar denotes 100 nm. (e) SEM image of the therapeutics coloaded AuNRsPSiNPs functionalized calcium alginate nanohydrogel. The scale bar denotes 200 nm.

they have a high loading capacity due to their high surface-area-to-volume ratio. By chemically modifying the PSi NPs surface group and conjugating them with targeting agents to increase cellular uptake,[6,9] PSi NPs have been shown to enhance delivery efficiency and reduce side effects due to improved localization in tumors. Gold nanorod (AuNR) is an FDA approved drug carrier and therapeutic agent; several AuNR based formulations are in phase I clinical trial. They are also often utilized in photothermal therapy[10,11] and in triggered drug release and photoacoustic imaging[10−12] due to their unique optical properties. However, therapeutics release from both PSi NPs and AuNRs is fast and not controllable within the body.[13,14]

Encapsulation of AuNRs conjugated PSi NPs within a biocompatible hydrogel shell overcomes the quick leakage limitation while enabling their advantages to be used in cancer therapy.[15] We synthesize novel gold nanorods conjugated porous silicon nanoparticles (AuNRsPSiNPs) cores with photothermal properties to coload hydrophobic and hydrophilic therapeutics and encapsulate them within a biocompatible calcium alginate hydrogel using water-in-oil microemulsion templates through cross-linking the shell (Scheme 1). We quantify the release profile of the AuNRsPSiNPs-in-calcium alginate nanocarriers for both hydrophilic and hydrophobic therapeutics. Finally, we demonstrate the nanocarriers' biomedical application in photothermal combination therapy.

We synthesize hydrophilic short gold nanorods about 50 nm in size, shown in the TEM micrograph in Figure 1a. Functional PSi NPs with carboxyl (COOH) surface groups are fabricated using electrochemical anodization,[7] yielding an average particle size of 129.2 ± 34.3 nm and zeta-potential of 63.01 ± 0.6 mV.

AuNRsPSiNPs are synthesized through a two-step reaction at 25 °C. The carboxyl groups of PSi NPs are reacted with the amine group of cysteamine (H_2NCHCH_2SH) through *N*-(3-

DOI: 10.1021/acs.nanolett.7b05210
Nano Lett. XXXX, XXX, XXX−XXX

(dimethylamino)propyl)-*N*′-ethylcarbodiimide hydrochloride (EDC) mediated reaction, after which the PSi-CON−$CHCH_2$−HS with HS surface groups is easily connected with the gold nanorods. The morphology of the AuNRsPSiNPs nanoparticles is shown by scanning electron microscopy (SEM) in Figure 1b. We use X-ray photoelectron spectroscopy (XPS) to confirm the successful formation of AuNRsPSiNPs, as shown by the C, N, O, S, Si, and Au peaks (Figure 1c).

We use biocompatible water-in-oil microemulsions as water core microreactors to produce calcium alginate hydrogel shells to encapsulate AuNRsPSiNPs that has been preloaded with therapeutics. AuNRsPSiNPs are first loaded with hydrophobic molecular targeting therapeutics, Afatinib, Docetaxel, or Erlotinib. Then, a mixture of hydrophilic antibody, therapeutic DOX,[16] and the AuNRsPSiNPs are dissolved in a 1−2 wt % sodium alginate solution, followed by mixing with a 0.3 M AOT-isooctane oil phase to form a w/o microemulsion. Finally, the w/o microemulsion is cross-linked by pump-controlled dropwise addition of another w/o microemulsion containing dilute $CaCl_2$ solution, as shown in Scheme 1. Images of calcium alginate nanohydrogels with and without AuNRs-S-PSi loaded with therapeutics, taken by SEM, are shown in Figure 1d,e, respectively. The nanohydrogel size can be controlled by tuning the molar ratio between the water and oil phases.[17] The diameter of nanohydrogels without nanoparticles is about 120 nm, while the diameter of nanohydrogels encapsulating nanoparticles is about 250 nm. Si, Au, S, and Ca peaks in the SEM-energy dispersive X-ray spectrum (Figure S1a) confirm the successful encapsulation of AuNRsPSiNPs within the calcium alginate nanohydrogel. The hydrodynamic diameter of the AuNRsPSiNPs functionalized calcium alginate nanohydrogel is measured by dynamic light scattering (DLS) at 298 K (Figure S1b).

To confirm the biocompatibility of the AuNRs-S-PSi nanoparticles and the AuNRsPSiNPs functionalized calcium alginate nanohydrogels, we expose MCF-7, SKBR-3, and MDA-MB-231 breast cancer cells to different concentrations of the nanocarriers and assess viability after 24 h of incubation at 37 °C. The cell viability rate decreases from 95% to 75% with increasing AuNRsPSiNPs concentrations from 50 μg/mL to 400 μg/mL (Figure 2a), and decreases from 95% to 80% with increasing AuNRsPSiNPs functionalized calcium alginate nanohydrogel concentrations from 100 μg/mL to 1000 μg/mL (Figure 2b). Notably, cell viability in the presence of 100 μg/mL nanohydrogel containing 10 nM AuNRs is 95.3 ± 3.8%. Calcium alginate nanohydrogel as the shell of the AuNRsPSiNPs is much more biocompatible than the AuNRsPSiNPs alone. All cell viability and cytotoxicity results confirm that the prepared AuNRsPSiNPs and AuNRsPSiNPs functionalized nanohydrogel are cytocompatible. Thus, they are potentially a suitable therapeutics codelivery nanocarrier for many biomedical applications.

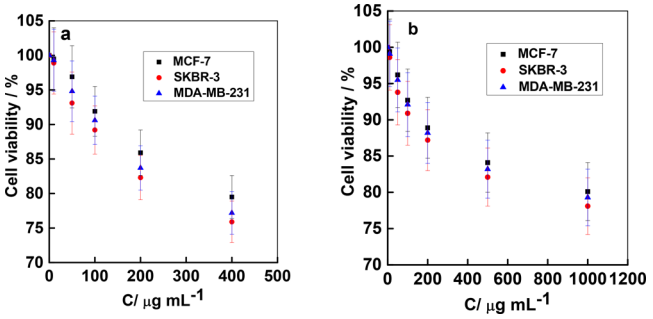

Figure 2. Biocompatibility study of AuNRsPSiNPs and AuNRsPSiNPs functionalized calcium alginate nano hydrogel on MCF-7, SKBR-3, and MDA-MB-231 cells at 310 K. (a) The cell viability of AuNRsPSiNPs on MCF-7, SKBR-3, and MDA-MB-231 cells after 24 h incubation at 310 K (10 nM AuNRs set up as control; n = 3, mean ± SD). (b) The cell viability of AuNRsPSiNPs functionalized calcium alginate nano hydrogel on MCF-7, SKBR-3, and MDA-MB-231 cells after 24 h incubation at 310 K (10 nM AuNRs within 200 μg/mL PSi set up as control; n = 3, mean ± SD).

The UV absorption curves for standard concentrations of DOX solutions, AuNRs, and the DOX- or AuNRs-loaded nanohydrogel solutions are measured at 488 and 975 nm using a UV−vis spectrophotometer. The initial and the total released concentration of hydrophobic therapeutics Afatinib and Docetaxel are measured by high-performance liquid chromatography (HPLC). The drug encapsulation efficiency and loading degree is then calculated based on the initial drug concentration and total release concentration. We find that the loading degree of hydrophobic therapeutics in AuNRsPSiNPs core is above 10% but the total decreases slightly after the nanohydrogel encapsulation step, while the loading degree of hydrophilic therapeutics in the nanohydrogel is about 10%.

In vitro dynamic dialysis release of therapeutics including DOX, antibody, Docetaxel, and Afatinib from free solution, PSi NPs, AuNRsPSiNPs, and AuNRsPSiNPs functionalized calcium alginate nanohydrogel into solutions imitating blood (PBS pH 7.4) and acidic tumor (pH 5.2) environments are carried out using a minidialysis kit at 37 °C. The release profile of DOX from free solution, PSi NPs and AuNRsPSiNPs into pH 7.4 and pH 5.2 phosphate buffered saline (PBS) solutions is shown in Figure 3a,b, and Figure S2. The in vitro release studies indicate that no initial burst release occurs and that 90−100% of the drug is released from the nanoparticles suspension into the release medium within 24 h. The release of DOX from the AuNRsPSiNPs suspension (80% of drug released at 12 h) is much slower than the dissolution profile of free DOX and the DOX release from PSi NP (80% of drug released at less than 2 h), possibly due to the ability of gold nanorods to bind hydrophilic drugs, thus delaying release. The release profile of therapeutics including DOX, Afatinib, Docetaxel, and antibody from AuNRsPSiNPs functionalized calcium alginate nanohydrogel into PBS pH 7.4 or pH 5.2 buffer solutions at 37 °C is shown in Figure 3c,d. The AuNRsPSiNPs encapsulated in calcium alginate nanohydrogel platform releases therapeutics much slowly than both PSi NPs and AuNRsPSiNPs, indicating successful protection of therapeutics by the calcium alginate shell (80% of drug released at 20 h at pH 7.4). Moreover, the therapeutics release rate increases in an acidic environment (80% of drug released at 12 h).

The plasmonic resonance peak of AuNRs is at 975 nm, which well distinguish them from the surrounding tissue and enable them for better biomedical applications. In addition, gold nanorods carrying hydrophilic therapeutics can also trigger release of DNA oligonucleotides[18] and anticancer drug doxorubicin with heat induced by laser irradiation. The in vitro release of DOX from the functionalized nanohydrogel into PBS buffer in the presence of gold nanorods under laser irradiation at 808 nm is much faster than the typical release rate of 24 h. Over 90% of DOX is released within 30 min (Figure 3e,f), indicating the potential of photothermal therapy using NIR laser irradiation.

DOI: 10.1021/acs.nanolett.7b05210
Nano Lett. XXXX, XXX, XXX−XXX

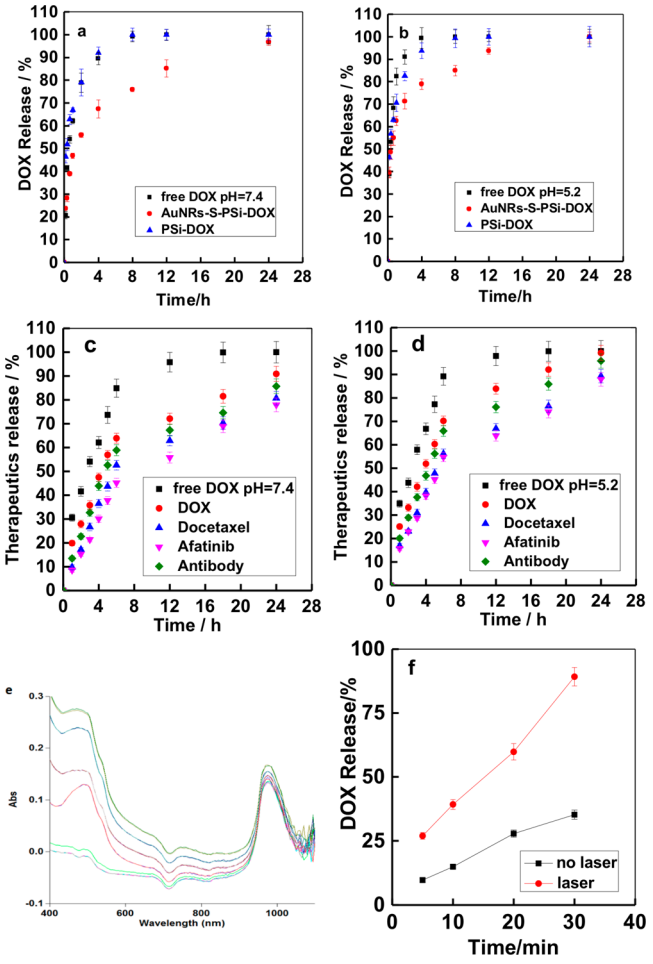

Figure 3. In vitro therapeutics release study. (a,b) Level of DOX from free solution, PSi NPs and AuNRsPSiNPs in PBS or pH 5.2 buffer containing 0.1 wt % Tween80 were release under magnetic stirring at various pH values. Each point represented the average of three measurements with standard deviation. (c) The in vitro therapeutics of DOX, Docetaxel, Afatinib, and antibody (488 nm fluorescent antibody) release from AuNRsPSiNPs functionalized calcium alginate nanohydrogel into PBS buffer containing 0.1 wt % Tween 80 at 310 K. Each point represented the average of three measurements with standard deviation. (d) The in vitro therapeutics of DOX, Docetaxel, Afatinib, and antibody (488 nm fluorescent antibody) release from AuNRsPSiNPs functionalized calcium alginate nanohydrogel into pH = 5.2 buffer containing 0.1 wt % Tween80 at 310 K. Each point represented the average of three measurements with standard deviation. (e,f) The UV−vis spectrum and the photothermal release of DOX (488 nm) and AuNRs (975 nm) from nanohydrogel under 808 nm laser irradiation at different time intervals and the photothermal effects on the release of DOX from nanoplatform under laser irradiation.

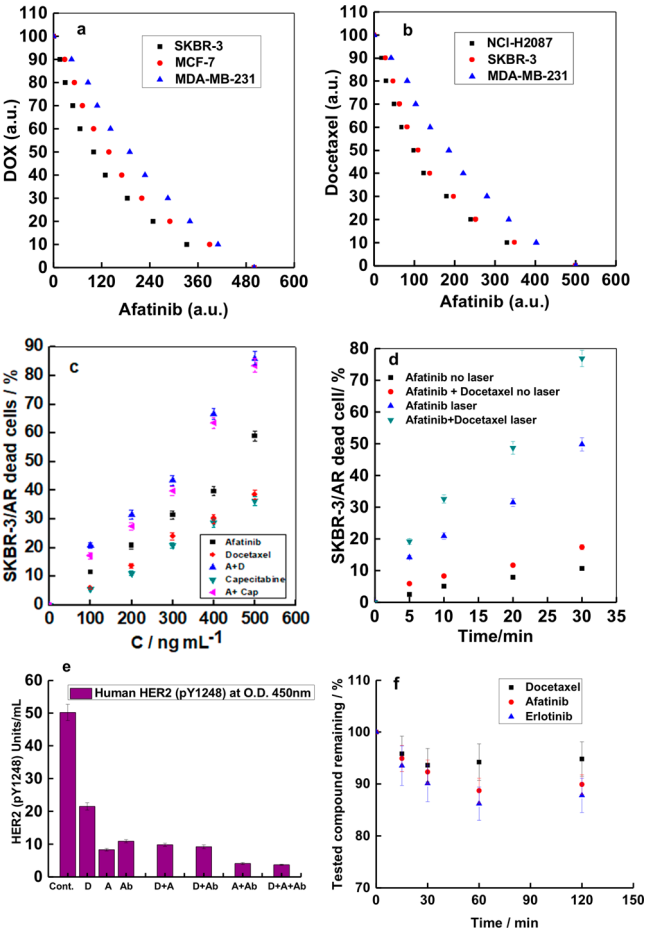

Figure 4. Synergism, multidrug resistance inhibition, HER2 (pY1248) and human plasma stability study. (a) The isobologram of two drugs combination of DOX+Afatinib on killing SKBR-3, MDA-MB-231 and MCF-7 cells at 37 °C. In the simulation, Afatinib has an I_{C50} (concentration giving 50% inhibition) of 500 au (arbitrary units), and I_{C50} of drug DOX is 100 au. (b) The isobologram of two drugs combination of Docetaxel and Afatinib on killing HER2 positive breast cancer SKBR-3 cells and EGFR positive nonsmall cell lung cancer NCl-H2087 cells, and breast cancer MDA-MB-231 cells at 37 °C. In the simulation, Docetaxel has an IC_{50} (concentration giving 50% inhibition) of 500 au (arbitrary units), IC_{50} of drug Afatinib is 100 au(c) The multidrug resistance inhibition on Afatinib-resistant SKBR-3/AR cells by Afatinib, Docetaxel, A+DCTX, Capecitabine and A + Cap loaded nanoplatform after 24 h incubation (C_A/C_{DCTX} = 1:1 and C_A/C_{Cap} = 1:1) at 310 K. (d) Cell viability of Afatinib, Afatinib +Docetaxel loaded nano hydrogel under laser irradiation at 808 nm at different time intervals or without laser irradiation on SKBR-3/AR cells after 2 h incubation using live/dead assay. (e) Human HER2 (pY1248) detection assay on HER2 positive breast cancer SKBR3 cells by anti-HER2 antibody (Ab), Afatinib (A), DOX(D), A+D, Ab+A, A +Ab, Ab+A+D after 16 h of treatment at 37 °C. (200 μ g/mL AuNRsPSiNPs functionalized calcium alginate nanohydrogel set as control; $C_{Afatinib}/C_D$ = 1:1; the concentration of anti-HER2 anitbody is 20 μg/mL; the total drugs concentration is 10 μ g/mL) (f) The human plasma stability of Docetaxel, Afatinib and Erlotinib from the AuNRs PSiNPs functionalized calcium alginate nanohydrogel. The percentage of parent compound remaining after incubation in human plasma is plotted versus incubation time. All incubations are performed in triplicated using 96 well cell culture plate. Each point represents the average of three measurements with standard deviation.

To demonstrate synergistic effects of the therapeutics combinations, we conduct in vitro cell viability study with several therapeutics alone and in combination on both HER2-positive and -negative breast cancer cells, and EGFR-positive nonsmall cell lung cancer (NSCLC) NCl-H2087 cells, shown in Figure 4a,b. The combinations do exhibit synergism:[19] adding a HER2/EGFR dual molecular-targeting drug Afatinib enhances treatment efficiency compared with using DOX alone against HER2/EGFR-positive cells. The combination of Afatinib and Docetaxel also behaves synergistically to induce more cell death in different cancer cell types.

Not only are the drug combinations more effective at inducing cell death, but they also have an added advantage of

DOI: 10.1021/acs.nanolett.7b05210
Nano Lett. XXXX, XXX, XXX−XXX

inhibiting multidrug resistance. We incubate Doxorubicin-resistant MCF-7/DOX cells (a model multidrug resistant breast cancer cell) and Afatinib-resistant SKBR-3/AR cells (HER2 positive multidrug resistant breast cancer cell) for 24 h at 37 °C in the presence of single drug solutions or nanocarriers loaded with therapeutics combinations. As shown in Figure 4c and Figure S3a−c, the cells are highly resistant to both DOX and Afatinib alone, but the therapeutic combinations cause enhanced cytotoxicity due to synergistic effects; moreover, at the same concentration, the therapeutic combinations are much more cytotoxic to drug-resistant cells than the individual therapeutics. In particular, Docetaxel significantly enhances killing of MCF-7/DOX or SKBR-3/AR cells when combined with DOX or Afatinib.

By incorporating photothermal treatment, the therapeutics can be delivered locally with high efficiency. We further perform in vitro cell viability testing on the MCF-7/DOX and SKBR-3/AR cells with and without 808 nm laser irradiation at different time intervals, followed by incubation for 2 h at 37 °C. The cytotoxicity rate remains relatively low without laser irradiation due to the slow natural release of therapeutics, as shown in Figure 4d and Figure S3d. However, laser irradiation dramatically increases cell death, especially with the therapeutic combination, after 30 min of laser irradiation. The AuNRs mediate the conversion of near-infrared radiation into heat, causing the fast release of therapeutics (see Figure S2) as well as a local temperature increase that thermally induces cell damage, while the released therapeutic combination functions to significantly inhibit multidrug resistance and promote cancer cell death. Using photothermal effects enables a quick, localized treatment procedure that avoids multidrug resistance for improved combination therapy. ATP assay using the same method according to our previous work[15] shows that therapeutics combination has synergism on HeLa cells, shown in Figure S4.

Treatment specificity can be further enhanced by including an anti-HER2 antibody. The quantify HER2(pY1248) protein in HER2-positive SKBR-3 breast cancer cells was detected using an ELISA assay, for which the cells treated with therapeutics for 16 h with and without anti-HER2 antibody in the nanohydrogel were lysed and analyzed. HER2-targeted therapeutics and the anti-HER2 antibody can effectively reduce HER2 (pY1248) expression alone, but the combination of Afatinib, Docetaxel and anti-HER2 antibody is the most effective formulation of the tested combinations to induce HER2-positive breast cancer cell death, as seen in Figure 4e.

Additionally, we quantify full-length HER2 and EGFR protein levels in lysates of HER2 positive SKBR-3 breast cancer cells and EGFR positive HeLa cells after 6 h of treatment with single drugs and drug combinations with and without anti-HER2/EFGR antibody. Figure S5 represents a clear decrease in HER2/EGFR protein levels after treatment by molecular targeting therapeutics and anti-HER2/EGFR antibody. Moreover, the HER2/EGFR targeting therapeutic and anti-HER2/EGFR antibody combination has high targeted killing selectivity which results in lowest HER2/EGFR protein level that irreversibly inhibits HER2/EGFR-positive cancer cells. Using Afatinib and Erlotinib, both EGFR targeting drugs, in combination further promotes EGFR-positive cancer cell death, while Docetaxel inhibits the cancer cell growth and migration.

Lastly, we perform a human plasma stability assay to determine the stability of the tested compounds (therapeutics Afatinib, Erlotinib, and Docetaxel) in plasma.[15] Within the AuNRsPSiNPs functionalized calcium alginate nanohydrogel, about 90% of the therapeutics remained after a 120 min incubation (Figure 4f). The therapeutics that are protected by AuNRsPSiNPs and the calcium alginate hydrogel shell are very stable in human plasma, suggesting potential for high performance in vivo and for clinical applications.

In conclusion, we demonstrate a novel biocompatible nanocarrier that codelivers therapeutics combinations with controllable release and photothermal properties for improved combination therapy. We synthesize gold nanorods conjugated porous silicon nanoparticles (AuNRsPSiNPs) and show that the AuNRsPSiNPs have a high loading capacity for therapeutics and their release can be controlled by the nanoparticles' photothermal properties. We successfully encapsulate the NPs within a calcium alginate nanohydrogel shell using water-in-oil microemulsion templates. These functionalized calcium alginate nanohydrogels exhibit excellent encapsulation efficiency, controllable release, low toxicity to normal cells, high loading capacity of therapeutics and photothermal properties. Moreover, we show that the therapeutics combinations significantly enhance cancer cell death and inhibit multidrug resistance through drug synergy and molecular targeting selectivity. Importantly, laser irradiation activates the nanoparticle photothermal properties to enable fast release of therapeutics and a local temperature increase for near-infrared laser photothermal therapy. Furthermore, incorporating anti-EGFR/HER2 antibody and EGFR/HER2 dual-targeted therapeutics more effectively reduces EGFR/HER2 protein expression when combined synergistically with one another or with other therapeutics. This work shows that a biocompatible nanocarrier comprised of gold nanorods conjugated porous silicon nanoparticles functionalized calcium alginate nanohydrogels holds great promise in the codelivery of various therapeutics with many properties suitable for biomedical applications, including multidrug-resistant cancer treatments and photothermal-assisted targeted combination therapy.

■ ASSOCIATED CONTENT

Supporting Information

The Supporting Information is available free of charge on the ACS Publications website at DOI: 10.1021/acs.nanolett.7b05210.

The gold nanorods conjugated porous silicon nanoparticles are synthesized in our lab, and the water-in-oil microemulsion templates are used to form functionalized calcium alginate nanohydrogels for coencapsulation and codelivery of various therapeutics and antibodies for advanced biomedical applications. Further detailed experimental procedures and supporting figures are provided (PDF)

■ AUTHOR INFORMATION

Corresponding Authors

*E-mail: mingtanhai@mater.ustb.edu.cn; mhai@seas.harvard.edu (M.H.).

*E-mail: weitz@seas.harvard.edu (D.W.). Phone: 001(617) 496-2842. Fax: 001(617) 495-0426.

ORCID

Zhou Yang: 0000-0003-1229-3739

Dong Chen: 0000-0002-8904-9307

Jarno Salonen: 0000-0002-5245-742X

DOI: 10.1021/acs.nanolett.7b05210
Nano Lett. XXXX, XXX, XXX−XXX

Hélder A. Santos: 0000-0001-7850-6309
David A. Weitz: 0000-0001-6678-5208

Present Addresses

○(H.K.) Cambridge International Curriculim Centre of Beijing Normal University, Beijing 100009, China, PR China.
◆(D.C.) College of Chemical and Biological Engineering, Zhejiang University, No. 38 Zheda Road, Hangzhou 310027, PR China.

Author Contributions

▽H.Z., Y.Z., L.Q., H.W., and H.K. have equal contribution to this work

Notes

The authors declare no competing financial interest.

■ ACKNOWLEDGMENTS

The authors are grateful to the Fundamental Research Funds for the Central Universities (No. FRF-BR-09-021B), 863 (No. 2006AA03Z108) program of China; NSF (DMR-1310266) and Harvard MRSEC (DMR-0820484) for financial support. H.Z. acknowledges Jane and Aatos Erkko Foundation (Grant 4704010), Academic of Finland (Grant 297580) and Sigrid Juselius Foundation (Grant 28001830K1) for financial support. H.A.S. acknowledges financial support from the Sigrid Juselius Foundation (Decision No. 4704580), and the European Research Council under the European Union's Seventh Framework Programme (FP/2007-2013, Grant No. 310892). Cell experiments, AFM, XPS, SEM, SEM-EDX, DLS, HPLC, TEM, laser irradiation, ATP and Human HER2/EGFR ELISA were conducted at the Harvard CNS and FAS center. We thank Timothy J. Cavanaugh at Harvard CNS for SEM-EDX measurement and Dr. Arthur McClelland at Harvard CNS for help with NIR laser irradiation experiments.

■ REFERENCES

(1) Jabir, N. R.; Tabrez, S.; Ashraf, G. M.; Shakil, S.; Damanhouri, G. A.; Kamal, M. A. *Int. J. Nanomed.* **2012**, *7*, 4391−4408.
(2) Kolishetti, N.; Dhar, S.; Valencia, P. M.; Lin, L. Q.; Karnik, R.; Lippard, S. J.; Langer, R.; Farokhzad, O. C. *Proc. Natl. Acad. Sci. U. S. A.* **2010**, *107* (42), 17939−17944.
(3) Torchilin, V. P. *Adv. Drug Delivery Rev.* **2006**, *58* (14), 1532−1555.
(4) Kong, F.; Zhang, X.; Zhang, H.; Qu, X.; Chen, D.; Servos, M.; Mäkilä, E.; Salonen, J.; Santos, H. A.; Hai, M.; Weitz, D. A. *Adv. Funct. Mater.* **2015**, *25* (22), 3330−3340.
(5) Park, J. H.; Gu, L.; von Maltzahn, G.; Ruoslahti, E.; Bhatia, S. N.; Sailor, M. J. *Nat. Mater.* **2009**, *8* (4), 331−336.
(6) Tasciotti, E.; Liu, X.; Bhavane, R.; Plant, K.; Leonard, A. D.; Price, B. K.; Cheng, M. M.; Decuzzi, P.; Tour, J. M.; Robertson, F.; Ferrari, M. *Nat. Nanotechnol.* **2008**, *3* (3), 151−157.
(7) Bimbo, L. M.; Denisova, O. V.; Mäkilä, E.; Kaasalainen, M.; De Brabander, J. K.; Hirvonen, J.; Salonen, J.; Kakkola, L.; Kainov, D.; Santos, H. A. *ACS Nano* **2013**, *7* (8), 6884−6893.
(8) Parodi, A.; Quattrocchi, N.; van de Ven, A. L.; Chiappini, C.; Evangelopoulos, M.; Martinez, J. O.; Brown, B. S.; Khaled, S. Z.; Yazdi, I. K.; Enzo, M. V.; Isenhart, L.; Ferrari, M.; Tasciotti, E. *Nat. Nanotechnol.* **2013**, *8* (1), 61−68.
(9) Wang, C. F.; Sarparanta, M. P.; Mäkilä, E. M.; Hyvonen, M. L.; Laakkonen, P. M.; Salonen, J. J.; Hirvonen, J. T.; Airaksinen, A. J.; Santos, H. A. *Biomaterials* **2015**, *48*, 108−118.
(10) Vigderman, L.; Khanal, B. P.; Zubarev, E. R. *Adv. Mater.* **2012**, *24* (36), 4811−4841.
(11) Huang, X.; Neretina, S.; El-Sayed, M. A. *Adv. Mater.* **2009**, *21* (48), 4880−4910.
(12) Kah, J. C. Y.; Chen, J.; Zubieta, A.; Hamad-Schifferli, K. *ACS Nano* **2012**, *6* (8), 6730−6740.
(13) Zhang, H.; Liu, D.; Shahbazi, M. A.; Mäkilä, E.; Herranz-Blanco, B.; Salonen, J.; Hirvonen, J.; Santos, H. A. *Adv. Mater.* **2014**, *26* (26), 4497−4503.
(14) Liu, D.; Zhang, H.; Fontana, F.; Hirvonen, J. T.; Santos, H. A. *Adv. Drug Delivery Rev.* **2017**, *26*, 1856−1883.
(15) Kong, F.; Zhang, H.; Qu, X.; Zhang, X.; Chen, D.; Ding, R.; Mäkilä, E.; Salonen, J.; Santos, H. A.; Hai, M. *Adv. Mater.* **2016**, *28* (46), 10195−10203.
(16) Tacar, O.; Sriamornsak, P.; Dass, C. R. *J. Pharm. Pharmacol.* **2013**, *65* (2), 157−170.
(17) Hai, M.; Kong, F. *J. Chem. Eng. Data* **2008**, *53* (3), 765−769.
(18) Zhang, H.; Qu, X.; Chen, H.; Kong, H.; Ding, R.; Chen, D.; Zhang, X.; Pei, H.; Santos, H. A.; Hai, M.; Weitz, D. A. *Adv. Healthcare Mater.* **2017**, *6* (20), 1700664.
(19) Kaelin, W. G., Jr. *Nat. Rev. Cancer* **2005**, *5* (9), 689−698.

DOI: 10.1021/acs.nanolett.7b05210
Nano Lett. XXXX, XXX, XXX−XXX